https://doi.org/10.1007/s41230-023-2143-1

Compression behavior of 316L lattice structures produced by indirect additive manufacturing

Yan-peng Wei[1,2], Hao Yang[3], Jing-chang Cheng[1], Peng Gao[1], Jian Shi[1], **Feng Lin[2], and *Bo Yu[1]

1. National Key Laboratory of Advanced Casting Technologies, Shenyang Research Institute of Foundry Co., Ltd. CAM, Shenyang 110022, China

2. Department of Mechanical Engineering, Tsinghua University, Beijing 100084, China

3. Key Laboratory of Space Physics, Beijing 100076, China

Abstract: As a new type of lightweight structure, metallic lattice structure has higher stiffness and strength to weight ratio. To freely obtain 316L lattice structures with designed cell structure and adjustable porosity, additive manufacturing combined with investment casting was conducted to fabricate the 316L lattice structures with Kelvin cell. The compression simulation of 316L lattice structures with different porosities was carried out by using the finite element method. The numerical simulation results were verified by compression experiment, and the simulated results were consistent with the compression tests. The compressive mechanical properties of 316L lattice structures are directly related to porosity and independent of strut diameters. The 316L lattice structures with Kelvin cell have a smooth stress-strain curve and obvious plastic platform, and the hump stress-strain curves are avoided.

Keywords: 316L lattice structures; indirect additive manufacturing; compression behavior; investment casting; finite element simulation

CLC numbers: TG142 **Document code:** A **Article ID:** 1672-6421(2023)02-083-06

1 Introduction

The metallic lattice structures show broad application prospects in aerospace, rail transportation, ships, and other fields because of their excellent structural characteristics such as specific strength and stiffness [1-3], and functional characteristics such as vibration and noise reduction [4-8], energy absorption [9-13], and so on. Its preparation methods mainly include investment casting [14-18], powder metallurgy method [19], deformation forming method [20], etc. For the preparation of nonferrous metallic lattice structures, such as aluminum and titanium lattice structures, the above methods are relatively mature, and some of them have achieved industrial applications [21]. However, due to the high melting point of steel materials, the preparation of 316L lattice structures has some problems, such as difficulty in controlling porosity and cell structures, and low degree of integration of structure and function. Additive manufacturing technology can prepare metallic lattice structures with complex cell structures [2, 22-25], realize the free design of cell structure and free control of porosity of metallic lattice structures [26], which provides a new solution for the preparation of 316L lattice structures. However, there are still several challenges to fabricate the metallic lattice structures using additive manufacturing, such as poor surface and anisotropic properties due to patterning mechanism, the selection of materials is limited, and so on. In this study, additive manufacturing combined with investment casting was implemented to fabricate 316L lattice structures, the fabrication method is also called indirect additive manufacturing [14, 16, 27].

In the research of the metallic lattice structures, various representative topological configurations were proposed. Among them, tetrahedron, pyramid [28, 29], and Kagome [30, 31] are the most widely used lattice unit cells. However, metallic lattice structures designed with the above-mentioned unit cells are generally anisotropic, the application conditions are limited and the applicability is insufficient. Therefore, it is an important research direction to find a lattice

***Bo Yu**

Male, born in 1963, Ph.D., Research Fellow. His research interests mainly focus on the development of advanced functional materials, design and fabrication of porous metals, and directional solidification process for superalloy turbine blade.

E-mail: Yub@chinasrif.com

**Feng Lin

E-mail: linfeng@tsinghua.edu.cn

Received: 2022-11-28; Accepted: 2022-12-30

structure that tends to be isotropic performance. Meanwhile, for the compression mechanical properties of the metallic lattice structures, the stress-strain curve of most metallic lattice structures shows the hump curve [10, 22, 32], few of them have smooth stress-strain curves and obvious plastic yield platform [33, 34]. To realize the integrated design of the structure and function of 316L lattice structures, it is necessary to design and prepare metallic lattice structures with a smooth stress-strain curve and an obvious plastic yield platform. In the research of porous materials, Kelvin once put forward the hypothesis that the tetrakaidecahedron is the ideal cell structure of porous materials, which has good spatial expansion and symmetry [35]. Luxner et al. [35] studied the anisotropy of the mechanical properties of lattice structures with different cell structures by numerical simulation, which showed that Kelvin's tetrakaidecahedron has good isotropy performance of the mechanical properties.

In this study, the Kelvin structure was selected as the unit structure of the 316L lattice structures, and the 316L lattice structures were obtained from additive manufacturing combined with investment casting. The compression behavior of the 316L lattice structures was studied using the finite element simulation and quasi-state compression test, and the compression stress-strain curves with different porosities of 316L lattice structures were established by using numerical simulation and experimental tests.

2 Finite element analysis model

The selection of matrix material is critical to metallic lattice structures. Fe-based materials have higher strength, stiffness, and corrosion resistance compared with nonferrous. The metallic lattice structures with Fe-based materials have a wide application space in lightweight and high temperature resistant components. Therefore, 316L stainless steel was chosen as the matrix material of metallic lattice structures in this study. The chemical composition of 316L stainless steel can be found in Table 1.

Table 1: Chemical composition of 316L stainless steel (wt.%)

Cr	Ni	Mo	Mn	Si	C	P	S	Fe
19.00	11.00	2.50	≤1.50	≤1.50	≤0.03	≤0.04	≤0.04	Bal.

The compression behavior of the 316L lattice structures was simulated by using the finite element method. The static performance of the 316L lattice structures contains the stress-stain curve, equivalent elastic modulus, equivalent yield strength, and so on. The equivalent elastic modulus and equivalent yield strength of the 316L lattice structures were calculated by finite element analysis with the static compression, and the bearing performance of 316L lattice structures was predicted based on the simulated and tested results.

The 316L lattice structures with the porosity of 70%, 80%, and 90% were used to carry out the static compression simulation, and the equivalent elastic modulus or yield strength of 316L lattice structures were studied by the compression stress-strain curve.

Figure 1 shows the finite element model diagram of the quasi-static compression simulation, the size of the metallic lattice structure is 51 mm×51 mm×51 mm, the strut diameter of the metallic lattice structures is 3 mm, the element size is set as 1 mm, and the total number of elements are 516,825. The 316L stainless steel was chosen as the matrix material of lattice structures, and the bilinear isotropic hardening model

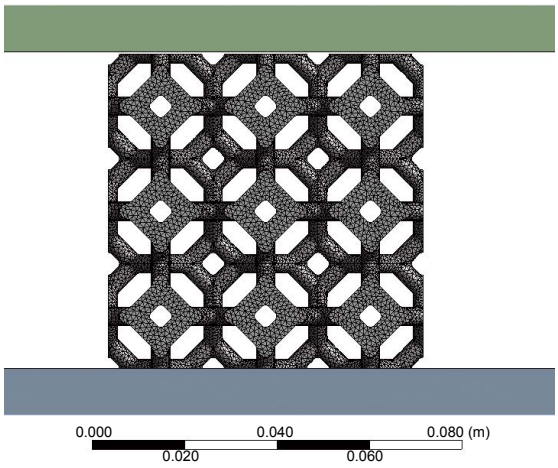

Fig. 1: Finite element model of 316L lattice structure under compression

was adopted to simplify the mechanical constitutive relation. The plastic performance of the stainless steel was simplified as a tangent, and the tangent modulus was set to 1.8×10^9 Pa in the finite element simulation. The static mechanical properties of the 316L stainless steel are shown in Table 2.

Table 2: Static mechanical properties of 316L stainless steel

Elastic modulus *E* (Pa)	Poisson's ratio *V*	Bulk modulus *K* (Pa)	Shear modulus *G* (Pa)	Yield strength *σ* (MPa)
1.93×10^{11}	0.31	1.69×10^{11}	7.37×10^{10}	210

In this finite element model, the stiffness behavior of the upper and lower pressing plates was set as the rigid body, the 316L lattice structures were set as the flexible body. The boundary condition of the lower plate was fixed support completely, and the load of the upper pressing plate was set as the displacement boundary. To ensure that the equivalent strain of the 316L lattice structures can reach more than 50%, so the displacement of the upper pressing plate was set as 35 mm. The type of the contact between pressing plates and 316L lattice structures was frictional contact, and the frictional coefficient was set to 0.25.

3 Experimental

The 316L lattice structures were fabricated by using additive manufacturing combining investment casting. The fabrication procedures consist the following steps: (1) prepare the precursor of the 316L lattice structures by selective laser sintering, the material for the selective laser sintering process was polystyrene; (2) prepare the casting mold on the basis of the precursor, using ceramic materials including quartz glass as the ceramic skeleton, fine silicon powder as the stabilizer, and silica sol as the binder; (3) fabricate the 316L lattice structures by using the vacuum gravity casting process: the preheating temperature of the ceramic preform was 930 °C, the pouring temperature was 1,550 °C, and the vacuum degree was less than 200 Pa; (4) remove the casting mold using potassium hydroxide in the high-pressure coreless kettle. The 316L lattice structure fabricated by additive manufacturing combined with investment casting is shown in Fig. 2. The strut diameters of the 316L lattice structure were 3 mm, 4 mm and 5 mm, respectively. The sizes of the 316 lattice structures were 119 mm×68 mm×68 mm, which can ensure the integrity of the compressed sample. The 316L lattice structures was solution treated at 1,080 °C for 2 h, and then water quenching before compression testing.

Compression testing was carried out on a DDL300 electronic universal testing machine to evaluate the static load-bearing properties of the solution treated 316L lattice structures. The compression speed was set as 1 mm·min^{-1} until the sample was compacted, and the force-displacement curve was obtained by the force and displacement sensor. The compression stress-strain curve of the 316L lattice structures was achieved from the force-displacement curve; the equivalent strain of the 316L lattice structures should reach 20% to ensure that a complete stress-strain curve can be obtained.

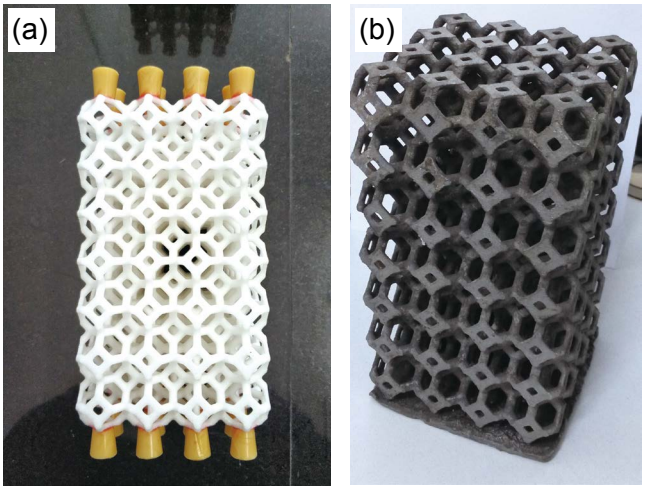

Fig. 2: Precursor (a) and sample (b) of 316L lattice structures fabricated by additive manufacturing combined with investment casting

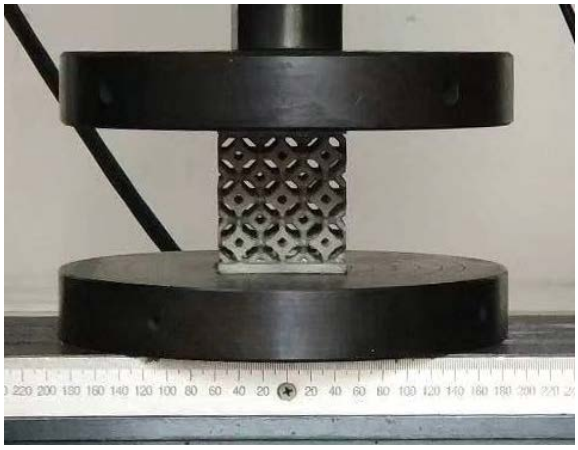

Fig. 3: Compression loading of 316L lattice structure

The compression performance test of the 316L lattice structures is different from the solid metal, and its performance is affected by the size of the sample. To eliminate the size effect, the 3×3×3 unit cell arrangement of the 316L lattice structures was used to conduct compression test according to the finite element analysis to ensure the accuracy of experiment results. Figure 3 shows the compression loading of the 316L lattice structure.

4 Results and discussion

4.1 Finite element analysis

Figure 4 shows the deformation contours of the 316L lattice structures under the static compression process. It can be seen from Fig. 4 that the deformation of the whole 316L lattice structure is uniform in the static compression process, the deformation and collapse of the unit cell occur simultaneously, and the plastic bending of the cell edges is the main deformation mode in the compression process.

The 316L lattice structures with different porosities were simulated by the finite element method under the static compression process, and the equivalent elastic modulus and equivalent yield strength of different porosities were achieved from the compression stress-strain curves of the 316L lattice structures. Some of the specimen parameters of 316L lattice structures are shown in Table 3.

Figure 5 shows the compression stress-strain curves of the 316L lattice structures with a strut diameter of 3 mm but different porosities from the simulated results. It can be seen that the 316L lattice structures have a smooth stress-strain curve and an obvious plastic platform. None of them shows the hump stress-strain curves. The compression stress-strain curves of the

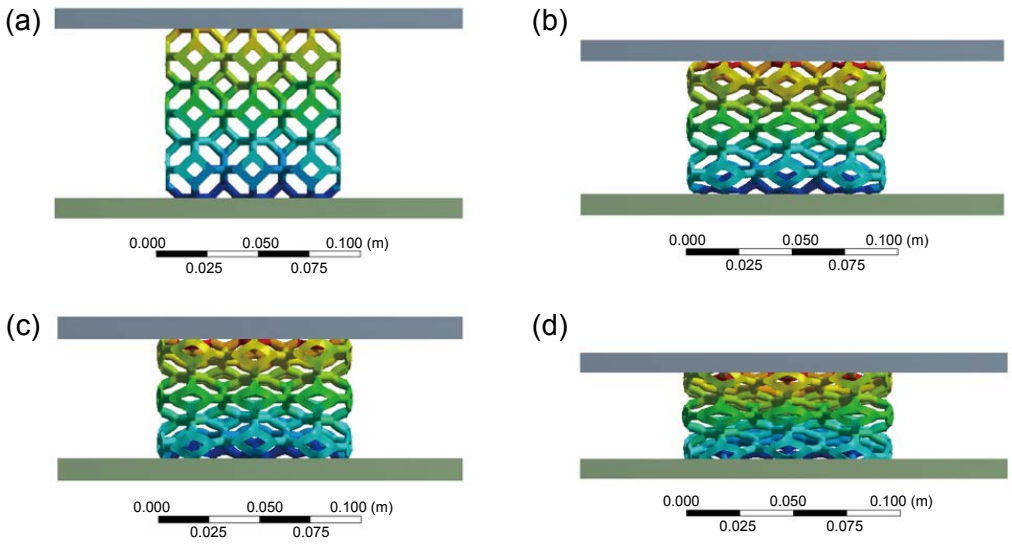

Fig. 4: Deformation contours of metallic lattice structures under the static compression process

Table 3: Parameters of 316L lattice structures

Sample No.	Length-to-diameter ratio	Porosity *P* (%)	Specimen size (mm)
1	1.5	70	38×38×38
2	2	80	51×51×51
3	2.5	90	64×64×64

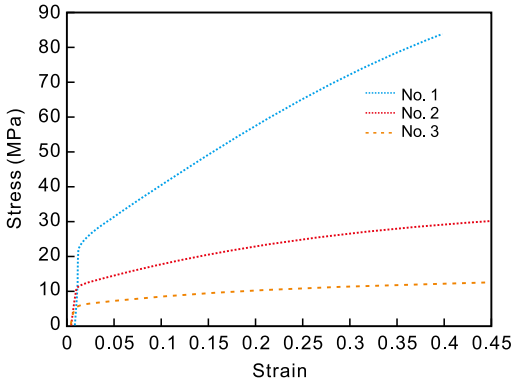

Fig. 5: Compression stress-strain curves of 316L lattice structure with a strut diameter of 3 mm but different porosities

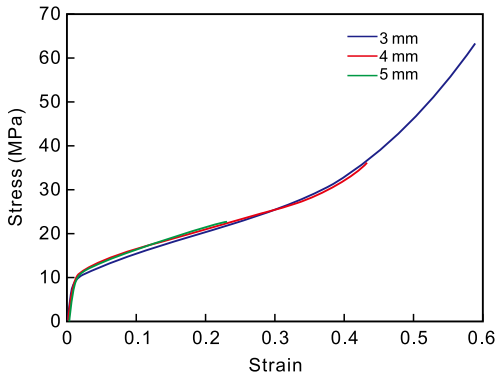

Fig. 6: Compression stress-strain curves of 316L lattice structures with the same porosity (80%) but different strut diameters

samples with different porosities are quite different, indicating that with the decrease of the porosity, the equivalent elastic modulus and equivalent yield strength of 316L lattice structures are obviously increased, which proved that porosity is one of the main factor influencing the compression properties of 316L lattice structures under the certain matrix materials.

4.2 Comparison of experiments and simulations

The compression deformation mode of the 316L lattice structures includes the following three steps: (1) overall uniform deformation in the quasi-static range; (2) structural collapse; (3) tends to be densification finally. After the compression, according to the force-displacement curve obtained from the experiment, the stress-strain curve of the 316L lattice structures with the same porosity but different pore sizes is shown in Fig. 6. The porosity of these 316L lattice structures was 80%. The strut diameters of the 316L lattice structures were 3 mm, 4 mm and 5 mm, respectively.

It can be seen from Fig. 6 that the compression stress-strain curves of the 316L lattice structures with the same porosity in the static compression process are coincident, and the trends of stress-strain curves are the same. It proves that the equivalent elastic modulus and equivalent yield strength of the 316L lattice structures are only related to the porosity for a certain matrix material, and have no obvious relationship with the strut diameters.

The compression speed of the three samples in the above experiment are all 1 mm·min^{-1}, but because the lengths of the

samples are different, the strain rates are also different. The strain rates of the three samples are 1.41×10^{-4}, 1.05×10^{-5} and 8.42×10^{-5}, respectively. It can be seen that the three samples are quasi-statically compressed at different strain rates, but their equivalent elastic modulus and equivalent yield strength are unchanged, indicating that the mechanical properties of the 316L lattice structures in the quasi-static range are not sensitive to strain rates.

It should be noted that the main reason for the different strain values (Fig. 6) is due to the limitations of the equipment (the maximum load of the equipment is 300 kN, which is not enough to fully compact the sample), the three samples cannot be guaranteed to reach the same strain, but the same compression is guaranteed. The speed also clearly characterizes the linear-elastic stage and the plastic yield stage of the static compression of the 316L lattice structures. Therefore, the three curves are fully applicable to this experiment.

The above experimental and simulated results are compared and analyzed, and the comparison curves are shown in Figs. 7 and 8. The strut diameters of the 316L lattice structures are 3 mm in Fig. 7 and 5 mm in Fig. 8.

From Figs. 7 and 8, it can be found that there is a common feature in the quasi-static compression simulation and experimental comparison charts, that is, the equivalent elastic modulus and equivalent yield strength of the simulation results are higher than the experimental results. This is mainly because there are no microscopic defects inside the material and no cracks on the surface in the numerical simulation. However, due to the characteristics of investment casting, there are a few shrinkage porosities inside the experimental sample and micro-cracks on the surface. Therefore, the experimental values were all lower than the simulated value.

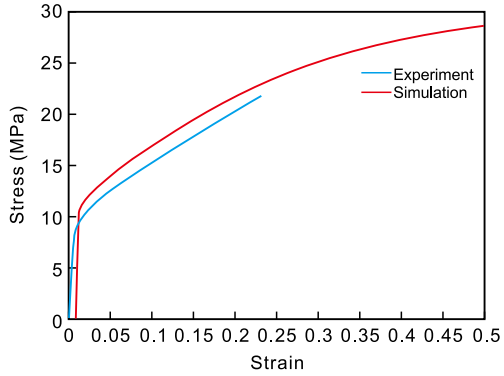

Fig. 7: Comparison of compression stress-strain curves between simulation and actual measurement of the 3 mm sample

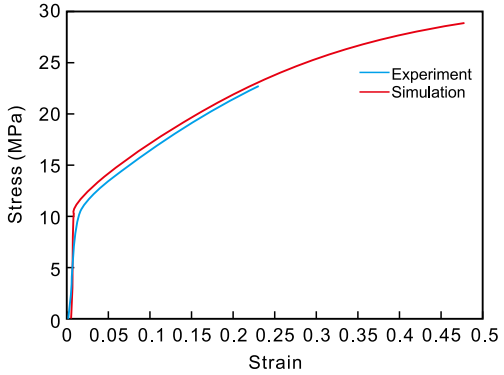

Fig. 8: Comparison of compression stress-strain curves between simulation and actual measurement of the 5 mm sample

As can be seen from Figs. 7 and 8, the two curves of the experiment and simulation are basically consistent, but during subsequent compression, the experimental curve begins to rise gradually, which eventually exceeds the simulated curve. In the stress-strain curve of the experiment in Fig. 7, a relatively obvious densification phenomenon appears after the strain reaches about 0.4, that is, the sample begins to be compacted, but the simulation results do not increase significantly. The main reason for this phenomenon is due to the heat treatment process of the experimental sample in the early stage. There is a great amount of oxide scale on the surface, which greatly increases the friction between the surfaces of the sample, so that the growth rate of the experimental compression force gradually increases. Finally, the simulation and experimental results are deviated. Nevertheless, it is not affected to obtain the equivalent elastic modulus and yield strength, because these performance paramaters were achieved in compression with linear elasticity stage.

It can be seen that the experimental and simulated curves are relatively consistent during static compression, indicating that the parameters set in the finite element simulation are accurate, and the results are credible. It also verifies that the 316L lattice structures with Kelvin cell have a smooth stress-strain curve and obvious plastic platform from the compression behavior, the hump curves are avoided and the application range of the metallic lattice structures is greatly broadened.

5 Conclusion

In this study, the 316L lattice structures with Kelvin unit cell were designed and fabricated by using additive manufacturing combined with investment casting. The compression behavior of the 316L lattice structures was studied by the finite element simulation and experimental testing. Results show that the simulated and experimental stress-strain curves are in good agreement with each other. The compression deformation mode of the 316L lattice structures consists overall uniform deformation in the quasi-static range, structural collapse and tend to be densification finally. The results show that the compressive mechanical properties of 316L lattice structures are directly related to porosity and independent of strut diameter size. The 316L lattice structures with Kelvin cell have a smooth stress-strain curve and obvious plastic platform, and the hump stress-strain curves are avoided.

Acknowledgement

This research work was supported by the Technology Development Fund of the China Academy of Machinery Science and Technology (No. 170221ZY01).

Conflict of interest

The authors declare that they have no conflict of interest.

References

[1] Xue Y, Wang X, Wang W, et al. Compressive property of Al-based auxetic lattice structures fabricated by 3-D printing combined with investment casting. Materials Science and Engineering: A, 2018, 722: 255–262.
[2] Köhnen P, Haase C, Bültmann J, et al. Mechanical properties and deformation behavior of additively manufactured lattice structures of stainless steel. Materials & Design, 2018, 145: 205–217.
[3] Carraturo M, Alaimo G, Marconi S, et al. Experimental and numerical evaluation of mechanical properties of 3d-printed stainless steel 316L lattice structures. Journal of Materials Engineering and Performance, 2021, 30: 5247–5251.
[4] Kim S, Lee C W. A review on manufacturing and application of open-cell metal foam. Procedia Materials Science, 2014, 4: 305–309.
[5] Potes F C, Silva J M, Gamboa P V. Development and characterization of a natural lightweight composite solution for aircraft structural applications. Composite Structures, 2016, 136: 430–440.
[6] Fiocchi J, Biffi C A, Scaccabarozzi D, et al. Enhancement of the damping behavior of Ti6Al4V alloy through the use of trabecular structure produced by selective laser melting. Advanced Engineering Materials, 2019, 22(2): 1900722.
[7] Syam W P, Wu J W, Zhao B, et al. Design and analysis of strut-based lattice structures for vibration isolation. Precision Engineering, 2018, 52: 494–506.
[8] Wei Y, Yu B, Yang Q, et al. Damping behaviors of steel-based kelvin lattice structures fabricated by indirect additive manufacture combining investment casting. Smart Materials and Structures, 2020, 29(5): 109331.
[9] Ajdari A, Nayeb-Hashemi H, Vaziri A. Dynamic crushing and energy absorption of regular, irregular and functionally graded cellular structures. International Journal of Solids and Structures, 2011, 48(3–4): 506–516.
[10] Jin N, Wang F, Wang Y, et al. Failure and energy absorption characteristics of four lattice structures under dynamic loading. Materials & Design, 2019, 169: 107655.
[11] Ozdemir Z, Tyas A, Goodall R, et al. Energy absorption in lattice structures in dynamics: Nonlinear fe simulations. International Journal of Impact Engineering, 2017, 102: 1–15.
[12] Ozdemir Z, Hernandez-Nava E, Tyas A, et al. Energy absorption in lattice structures in dynamics: Experiments. International Journal of Impact Engineering, 2016, 89: 49–61.
[13] Hawreliak J A, Lind J, Maddox B, et al. Dynamic behavior of engineered lattice materials. Scientific Reports, 2016, 6: 28094.
[14] Mun J, Ju J, Thurman J. Indirect additive manufacturing based casting of a lattice structure. In: Proceedings of the ASME 2014 International Mechanical Engineering Congress and Exposition, Canada, 2014.
[15] Snelling D, Li Q, Meisel N, et al. Lightweight metal cellular structures fabricated via 3d printing of sand cast molds. Advanced Engineering Materials, 2015, 17(7): 923–932.
[16] Mun J, Yun B G, Ju J, et al. Indirect additive manufacturing based casting of a periodic 3D cellular metal – flow simulation of molten aluminum alloy. Journal of Manufacturing Processes, 2015, 17: 28–40.
[17] Carneiro V H, Rawson S D, Puga H, et al. Additive manufacturing assisted investment casting: A low-cost method to fabricate periodic metallic cellular lattices. Additive Manufacturing, 2020, 33: 101085.
[18] Pinto P, Peixinho N, Silva F, et al. Compressive properties and energy absorption of aluminum foams with modified cellular geometry. Journal of Materials Processing Technology, 2014, 214(3): 571–577.
[19] Youn S W, Kang C G. Fabrication of foamable precursors by powder compression and induction heating process. Metallurgical and Materials Transactions: B, 2004, 35: 769–776.
[20] Wadleya H N G, Fleckb N A, Evansc A G. Fabrication and structural performance of periodic cellular metal sandwich structures. Composites Science and Technology, 2003, 63(16): 2331–2343.
[21] Ashby M F, Evans A G, Fleck N A, et al. Metal foams: A design guide. Oxford: Butterworth-Heinermann, 2000.
[22] White B C, Garland A, Alberdi R, et al. Interpenetrating lattices with enhanced mechanical functionality. Additive Manufacturing, 2021, 38: 101741.
[23] Yang K, Wang J, Jia L, et al. Additive manufacturing of Ti-6Al-4V lattice structures with high structural integrity under large compressive deformation. Journal of Materials Science & Technology, 2019, 35(2): 303–308.
[24] Xu Y D, Zhang H Z, Savija B, et al. Deformation and fracture of 3d printed disordered lattice materials: Experiments and modeling. Materials & Design, 2019, 162: 143–153.
[25] Tang S Y, Yang L, Fan Z T, et al. A review of additive manufacturing technology and its application to foundry in China. China Foundry, 2021, 18(4): 249–264.
[26] Wang X, Xu S, Zhou S, et al. Topological design and additive manufacturing of porous metals for bone scaffolds and orthopaedic implants: A review. Biomaterials, 2016, 83: 127–141.
[27] Almonti D, Baiocco G, Tagliaferri V, et al. Design and mechanical characterization of voronoi structures manufactured by indirect additive manufacturing. Materials (Basel), 2020, 13(5): 1085.
[28] Huang Y, Xue Y, Wang X, et al. Mechanical behavior of three-dimensional pyramidal aluminum lattice materials. Materials Science and Engineering: A, 2017, 696: 520–528.
[29] Sun Y, Gao L. Mechanical behavior of all-composite pyramidal truss cores sandwich panels. Mechanics of Materials, 2013, 65: 56–65.
[30] Wang R, Shang J Z, Li X, et al. Vibration and damping characteristics of 3D printed Kagome lattice with viscoelastic material filling. Scientific Reports, 2018, 8: 9604.
[31] Wei Y P, Yu B, Yang Q Z, et al. Numerical simulation and experimental validation on fabrication of nickel-based superalloy kagome lattice sandwich structures. China Foundry, 2020, 17(1): 21–28.
[32] Choy S Y, Sun C N, Leong K F, et al. Compressive properties of functionally graded lattice structures manufactured by selective laser melting. Materials & Design, 2017, 131: 112–120.
[33] Liu C, Lertthanasarn J, Pham M S. The origin of the boundary strengthening in polycrystal-inspired architected materials. Nature Communications, 2021, 12(1): 4600.
[34] Alomar Z, Concli F. Compressive behavior assessment of a newly developed circular cell-based lattice structure. Materials & Design, 2021: 109716.
[35] Luxner M H, Stampfl J, Pettermann H E. Numerical simulations of 3D open cell structures – influence of structural irregularities on elasto-plasticity and deformation localization. International Journal of Solids and Structures, 2007, 44(9): 2990–3003.